Loss of sphingosine kinase 2 enhances Wilm's tumor suppressor gene 1 and nephrin expression in podocytes and protects from streptozotocin-induced podocytopathy and albuminuria in mice

Faik Imeri [a], Bisera Stepanovska Tanturovska [a], Stephanie Schwalm [b], Sarbari Saha [b], Jinyang Zeng-Brouwers [b], Herrmann Pavenstädt [c], Josef Pfeilschifter [b], Liliana Schaefer [b] and Andrea Huwiler [a]

***a* - Institute of Pharmacology,** *University of Bern, Inselspital, INO-F, Bern CH-3010, Switzerland*
***b* - Pharmazentrum Frankfurt,** *Institute of Pharmacology and Toxicology, Goethe University, Frankfurt am Main D-60590, Germany*
***c* - Medizinische Klinik D,** *University Hospital Münster, Münster D-48149, Germany*

Corresponding to Andrea Huwiler: *Institute of Pharmacology, University of Bern, Inselspital, INO-F, Bern CH-3010, Switzerland. Huwiler@pki.unibe.ch, schaefer@med.uni-frankfurt.de.*
https://doi.org/10.1016/j.matbio.2021.05.003

Abstract

The sphingosine 1-phosphate (S1P) is a bioactive sphingolipid that is now appreciated as key regulatory factor for various cellular functions in the kidney, including matrix remodeling. It is generated by two sphingosine kinases (Sphk), Sphk1 and Sphk2, which are ubiquitously expressed, but have distinct enzymatic activities and subcellular localizations. In this study, we have investigated the role of Sphk2 in podocyte function and its contribution to diabetic nephropathy. We show that streptozotocin (STZ)-induced nephropathy and albuminuria in mice is prevented by genetic depletion of Sphk2. This protection correlated with an increased protein expression of the transcription factor Wilm's tumor suppressor gene 1 (WT1) and its target gene nephrin, and a reduced macrophage infiltration in immunohistochemical renal sections of STZ-treated Sphk2$^{-/-}$ mice compared to STZ-treated wildtype mice.

To investigate changes on the cellular level, we used an immortalized human podocyte cell line and generated a stable knockdown of Sphk2 (Sphk2-kd) by a lentiviral transduction method. These Sphk2-kd cells accumulated sphingosine as a consequence of the knockdown, and showed enhanced nephrin and WT1 mRNA and protein expressions similar to the finding in Sphk2 knockout mice. Treatment of wildtype podocytes with the highly selective Sphk2 inhibitor SLM6031434 caused a similar upregulation of nephrin and WT1 expression. Furthermore, exposing cells to the profibrotic mediator transforming growth factor β (TGFβ) resulted on the one side in reduced nephrin and WT1 expression, but on the other side, in upregulation of various profibrotic marker proteins, including connective tissue growth factor (CTGF), fibronectin (FN) and plasminogen activator inhibitor (PAI) 1. All these effects were reverted by Sphk2-kd and SLM6031434. Mechanistically, the protection by Sphk2-kd may depend on accumulated sphingosine and inhibited PKC activity, since treatment of cells with exogenous sphingosine not only reduced the phosphorylation pattern of PKC substrates, but also increased WT1 protein expression. Moreover, the selective stable knockdown of PKCδ increased WT1 expression, suggesting the involvement of this PKC isoenzyme in WT1 regulation.

The glucocorticoid dexamethasone, which is a treatment option in many glomerular diseases and is known to mediate a nephroprotection, not only downregulated Sphk2 and enhanced cellular sphingosine, but also enhanced WT1 and nephrin expressions, thus, suggesting that parts of the nephroprotective effect of dexamethasone is mediated by Sphk2 downregulation.

Altogether, our data demonstrated that loss of Sphk2 is protective in diabetes-induced podocytopathy and can prevent proteinuria, which is a hallmark of many glomerular diseases. Thus, Sphk2 could serve as a new attractive pharmacological target to treat proteinuric kidney diseases.

Introduction

Sphingosine 1-phosphate (S1P) is a bioactive lipid that has attracted overwhelming interest during the last decades due to its key regulatory role in many physiological and pathophysiological processes such as cell proliferation and survival, migration, inflammatory reactions, and extracellular matrix (ECM) remodeling [1-3]. Most of the actions of S1P are mediated by activation of cell surface S1P receptors, of which five subtypes have been identified, denoted as $S1P_{1-5}$ [4,5]. These receptors bind S1P with high affinity, couple to various G proteins, including $G_{i/0}$, G_q and $G_{12/13}$, and thereby stimulate a complex signal transduction network that finally determines the cells' response [4,6]. Since every cell type and organ tissue so far studied, expresses one or several S1PR subtypes, S1P is expected to influence many organs in a unique way, either as part of physiological processes or as part of pathological processes depending on the overall S1PR expression profile.

S1P is produced intracellularly by two sphingosine kinases (Sphk) [7,8,3,9], Sphk1 and Sphk2, and is degraded reversibly by either specific S1P phosphatases or unspecific lipid phosphatases to regenerate sphingosine, or irreversibly by the S1P lyase to hexadecenal and phosphoethanolamine [10]. The latter reaction is the only way to eliminate sphingolipids in the cell.

For each subtype of Sphk, several splice variants exist although their relevance and functions are largely unclear [7,11]. Although Sphk1 and Sphk2 enzymatically catalyze the same reaction, they show differential properties in substrate specificities, subcellular localizations and cellular functions [7]. While Sphk1 has a narrow substrate preference and phosphorylated sphingosine, dihydro-sphingosine and 4,8-sphingadienine, Sphk2 shows a broader substrate acceptance and also phosphorylates phytosphingosine and synthetic sphingosine-like structures including the immunomodulatory drug fingolimod, and other synthetic fingolimod derivatives [2].

Since potent and selective Sphk1 and Sphk2 inhibitors have only recently become available, in the past, genetic knockout mice of Sphk1 and Sphk2 have served as most useful tools to unravel subtype specific functions [12-14]. Neither the single depletion of Sphk1 or Sphk2 reveals an obvious phenotype, while a double knockout of both enzymes is embryonically lethal resembling the phenotype of systemic $S1P_1$ depletion [15]. However, on the molecular and lipid level, changes were clearly detected in both Sphk1 and Sphk2 deficient mice [16]. Thus, loss of Sphk1 resulted in 50% reduction of serum S1P levels, while loss of Sphk2 showed rather an increased serum level of S1P, suggesting that serum S1P mainly derives from Sphk1, whereas Sphk2 could be involved in serum S1P clearance that mainly occurs in the liver [17].

The kidney is a key organ responsible for blood filtration and elimination of toxic substances and drugs. Blood ultrafiltration is maintained by glomerular visceral epithelial cells, also called podocytes, which are highly differentiated cells and show a dense network of branched protrusions, that cover the whole filtration surface area. These protrusions are called foot processes which interdigitate and thereby form the slit diaphragm [18]. On the molecular level, the slit diaphragm is built by homo- and heterophilic interactions of a complex of podocyte-specific cell surface and intracellular molecules, including nephrin, podocin, NEPH1, CD2AP, and the actin cytoskeleton, which thereby regulate foot process morphology and actin dynamics. In many glomerular diseases, podocytes retract their foot processes, also known as foot process effacement, and this leads to a breakdown of the glomerular filtration barrier, to increased proteinuria and ultimately to end-stage renal disease and renal failure [19,20]. Besides the function of podocytes in blood filtration, they also contribute to ECM production in glomerulosclerosis and chronic kidney disease [19,21,22] and it is noteworthy that therapeutics, that are used to treat chronic kidney disease and a nephrotic syndrome, directly affect podocytes [23-26].

Previous studies have suggested a contribution of Sphk2 to renal tubulointerstitial fibrosis, and the loss of Sphk2 in mice mediates a protection from interstitial fibrosis [27-29], while the systemic overexpression of Sphk2 in a transgene mouse model, aggravated interstitial fibrosis induced by ureter ligation [28]. The mechanism of protection mediated by loss of Sphk2 remains inconclusive and may involve enhanced interferon γ production [27], increased Smad7 expression [28] or a dampening of the preceeding phase of immune cell infiltration and inflammation [28,29].

In the present study, we investigated the role of Sphk2 in podocytes, and its contribution to dysregulation of ultrafiltration and albuminuria in vivo, and in

a fibrotic sequela causing glomerulosclerosis. We used an immortalized human podocyte cell line to downregulate Sphk2 and found on the molecular level, a striking upregulation of the Wilm's tumor suppressor gene 1 (WT1) and its target gene nephrin. Furthermore, in a mouse model of streptozotocin-induced diabetic nephropathy, Sphk2 deficient mice were protected from diabetes-induced albuminuria, and this coincided with increased nephrin and WT1 expression in kidney sections of Sphk2 deficient mice. In addition, the well-known nephroprotective glucocorticoid dexamethasone, which is often used as first choice therapy in glomerulonephritis and various forms of nephrotic syndrome, not only upregulated nephrin and WT1, but also downregulated Sphk2 which may account for at least parts of glucocorticoids nephroprotective effects. These data suggest that Sphk2 downregulation represents an attractive approach to enhance nephrin expression which leads to a stabilization of podocyte's foot processes and ameliorates albuminuria in the disease model.

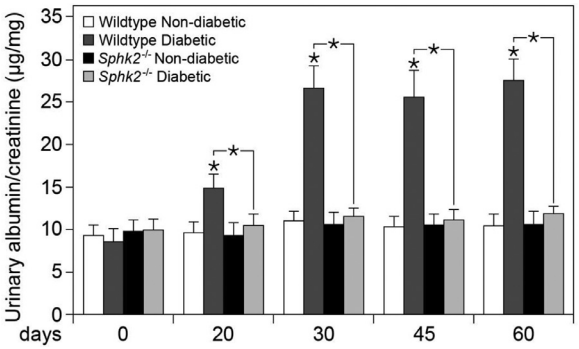

Fig 1. Effect of STZ-induced diabetic nephropathy in wildtype and *Sphk2*$^{-/-}$ mice on urinary albumin excretion. Urinary albumin excretion normalized to creatinine levels in the urine from wildtype/non-diabetic (white bars), wildtype/diabetic (dark gray bars), *Sphk2*$^{-/-}$/non-diabetic (black bars), and *Sphk2*$^{-/-}$/diabetic mice (light gray bars), before induction of diabetes mellitus (day 0), as well as 20, 30, 45, and 60 days after the last streptozotocin (STZ) injection. Albumin and creatinine were quantified as described in the Methods Section. Data are given as means ± SEM; $n = 6$; $^{*}p < 0.05$.

Results

Sphk2$^{-/-}$ mice are protected from STZ-induced albuminuria

Since Sphk2 deficiency has previously been shown to protect from fibrosis in various mouse models of tubulointerstitial fibrosis [27-29], we here investigated the role of Sphk2 in diabetic nephropathy, which is characterized by an initial glomerular injury including podocytopathy, glomerulonephritis and glomerulosclerosis, with only a secondary involvement of the tubular system. Wildtype and Sphk2 deficient mice were injected with the diabetogenic drug streptozotocin to kill pancreatic β-cells [30], which in turn, leads to hypoinsulinemia and hyperglycemia, and in the kidney to glomerular hyperfiltration, damage of podocytes and increased albuminuria [31]. Clinical parameters of this diabetes model are shown in suppl. Table S1, and reveal that blood glucose concentration was significantly enhanced in diabetic mice as compared to the control non-diabetic mice, while no difference was seen between control and Sphk2$^{-/-}$ mice in healthy state and disease induction. STZ-induced diabetes in control mice resulted in a time-dependent increase of albumin in the urine which was first detectable 20 days post-STZ and then constantly increased up to day 60 post-STZ, the end point of the experiment (Fig. 1). Remarkably, Sphk2$^{-/-}$ mice showed no significant albuminuria up to day 60 (Fig. 1), suggesting that loss of Sphk2 exerts a protection on the glomerular filtration barrier and prevents albuminuria. Staining of kidney sections at day 60 of the experiment revealed a markedly increased protein expression of the podocyte-specific protein nephrin in Sphk2$^{-/-}$ compared to wildtype healthy kidneys (Fig. 2A, upper row panels; and 2B). In diabetic kidneys, nephrin staining was reduced in both wildtype and Sphk2$^{-/-}$ as compared to the non-diabetic kidneys (Fig. 2B), but was still significantly higher in knockout than in wildtype kidneys. This phenomenon can be explained by the fact, that during the course of the disease, podocytes detach and are lost into the urine [32-34]. Notably, reduced nephrin expression is a hallmark of many glomerular diseases characterized by albuminuria [35].

Since nephrin expression is known to depend on the transcription factor Wilm's tumor suppressor gene 1 (WT1) [36,37], we also stained for this podocytic transcription factor. WT1 staining resembled the nephrin staining and was basally increased in Sphk2$^{-/-}$ compared to wildtype (Fig. 2A, lower row panels, and Fig. 2C). In diabetic animals, again, WT1 expression was reduced due to the loss of podocytes. The increased protein expression of nephrin and WT1 in Sphk2$^{-/-}$ kidneys was further confirmed in Western blot analyses of kidney lysates (Fig. 3A-C).

Next, we addressed the effect of Sphk2 deficiency on renal infiltration of macrophages by using immunostaining for the macrophage marker F4/80. In the tubulointerstitium from wildtype and Sphk2$^{-/-}$ diabetic kidneys (day 60 post-STZ), we found enhanced number of F4/80^{+} cells (suppl. Fig. S1). In agreement with our previous findings [28], this induction of infiltrating macrophage number was markedly

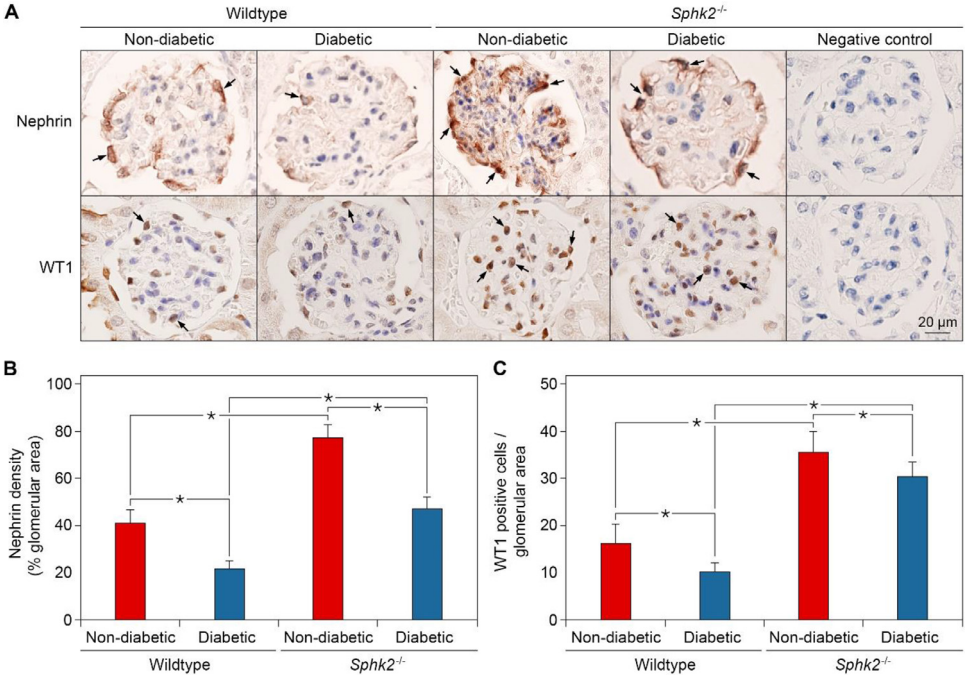

Fig 2. Immunohistochemical detection of nephrin and WT1 in renal glomeruli of non-diabetic and STZ-induced diabetic wildtype and *Sphk2*$^{-/-}$ mice. (A) Representative immunostaining (brown, depicted by arrows) for nephrin (upper panel) and WT1 (lower panel) in glomeruli of non-diabetic and diabetic wildtype and *Sphk2*$^{-/-}$ mice at days 60 post-STZ. Original magnification x400, Scale bars: 20 µm. (B and C) Density quantification of nephrin-positive area (% of glomerular area) (B) and quantification of WT1 positive cell numbers per glomerular area (mm^2) (C). All results are representative of 4 sets of experiments with 6 animals in each group. Data are given as means ± SEM. *$p < 0.05$.

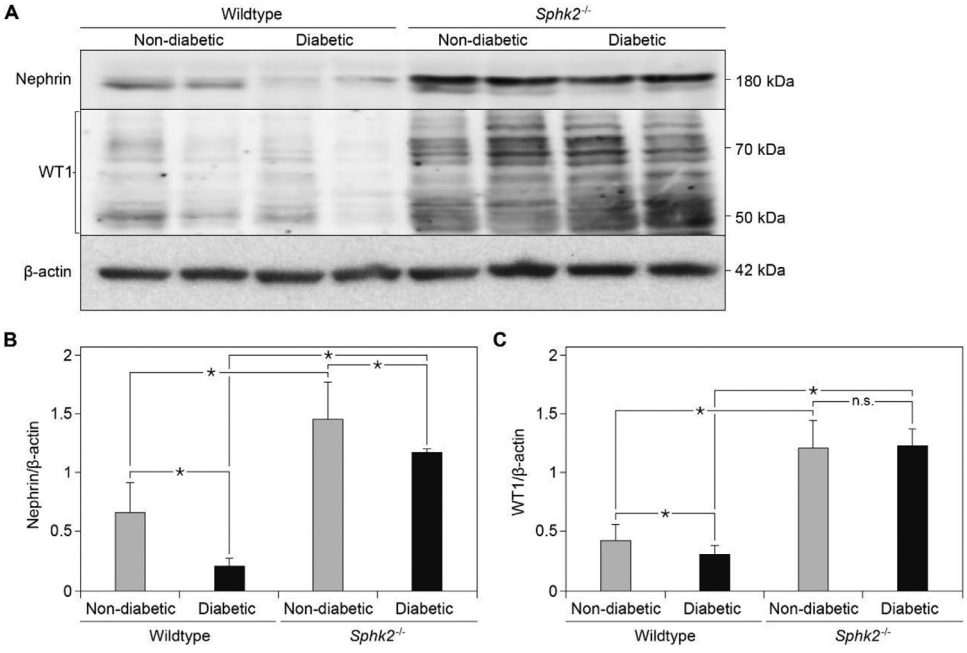

Fig 3. Nephrin and WT1 abundance in renal cortical homogenates of non-diabetic and STZ-induced diabetic wildtype and *Sphk2*$^{-/-}$ mice. (A-C) Representative Western blots (A) and the quantification for nephrin (B) and WT1 (C) in homogenates of renal cortex at days 60 post-STZ. All protein bands with a range from 50 to 75 kDa resulting from the WT1 alternative splicing are quantified densitometrically. β-actin was used as loading control. Data are given as means ± SEM; for at least $n = 4$; *$p < 0.05$.

reduced in diabetic kidneys from Sphk2$^{-/-}$ compared to wildtype mice (suppl. Fig. S1). We did not detect enhanced macrophage infiltration into glomeruli, which however may also be due to the very later time point (day 60) after disease induction.

Sphk2 knockdown in human podocytes or its catalytic inhibition upregulates nephrin and WT1 expression

To see whether the increased expression of nephrin and WT1, seen in kidneys of Sphk2$^{-/-}$ mice irrespective of disease induction or not, is reproduced in a cellular system, we used an immortalized human podocyte cell line, that is based on the introduction of a temperature-sensitive large T cell antigen. A stable Sphk2 knockdown was generated by transducing cells with lentiviral particles containing shRNA against Sphk2 or a control. The knockdown efficiency was determined on the mRNA and protein level by quantitative PCR analysis and Western blot analysis, respectively. As shown in Fig. 4, Sphk2 mRNA expression was reduced by 75% (Fig. 4A) while protein expression was completely abolished (Fig. 4B). However, the size of Sphk2 protein is not identical to the previously described size of 65.2 kDa [38]. A prominent double band is seen at 50−55 kDa which is lost in Sphk2-kd cells. In this context, it must be noted that 4 different isoforms and variants of Sphk2 exist, denoted as Sphk2 a, b, c, d [39]. While isoforms Sphk2 a and b have been confirmed and characterized on protein levels, isoforms c and d have still not been confirmed on protein level in any cell type, but are only listed in GenBank [39,40]. Notably, variant X5 (isoform d) results in the translation of an approx. 50 kDa protein, which is detected by the herein generated anti-hSphk2 antibody. Therefore, from our data we suggest that human podocytes mainly express the variant X5 of Sphk2d. We have further determined the functional consequence of Sphk2-kd by quantifying cellular sphingosine levels by mass spectrometry. As expected from loss of Sphk2, sphingosine levels significantly increased compared to control cells (Fig. 4C). An even stronger increase was seen when cells were treated for 20 h with the potent and highly selective Sphk2 catalytic inhibitor SLM6031434 [41] (Fig. 4C). No other sphingolipids were significantly changed by Sphk2-kd, with the exception of glucosyl-C16-ceramide being slightly but significantly reduced (suppl. Fig. S2).

Sphk2-kd cells were further characterized for expression of nephrin. In SDS-PAGE, nephrin runs at different sizes, i.e. 185 kDa, 135 kDa and 100 kDa, which is due to splice variants and multiple glycosylations [32]. The calculated mass of nephrin is 134 kDa, but the protein often appears at approximately 185−190 kDa which is hypothesized to be due to glycosylation at multiple sites [32]. In addition, a variant, denoted nephrin-α exists, that lacks exon 24 which codes for the whole transmembrane domain [32]. Nephrin has also been reported to be subject to protease cleavage, and two cleavage sites at amino acid residues 112 and 317 have been shown [42], yielding possible fragments of 120 and

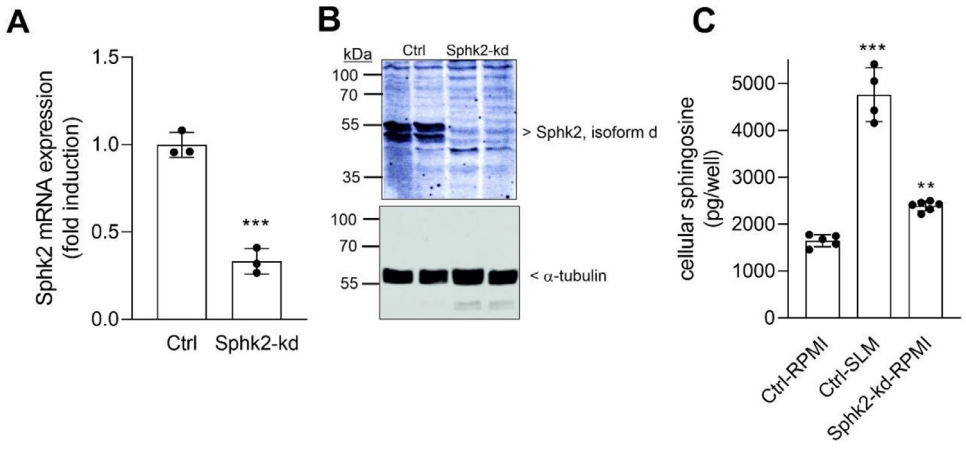

Fig 4. Characterization of stable Sphk2 knockdown in human podocytes. Confluent human podocytes, stably transduced with lentiviral particles containing an empty lentiviral vector (Ctrl) or a lentiviral vector containing Sphk2 shRNA (Sphk2-kd), were incubated for 20 h in serum-free RPMI. RNA and proteins were extracted and taken for quantitative PCR analysis of Sphk2 (A) or Western blot analysis of Sphk2 (B, upper panel) and the house-keeping protein α-tubulin (B, lower panel). (C) Control (Ctrl) and Sphk2-kd cells in 35-mm dishes were incubated for 20 h in serum-free RPMI in the absence (RPMI) or presence of SLM6031434 (1 μM, SLM), and lipids were extracted and processed for LC-MS/MS to quantify cellular sphingosine as described in the Methods section. Results in A are expressed as fold induction compared to ctrl-transduced cells and are means ± *S*.D. (n = 3). Results in C are expressed as pg/well and are means ± *S*.D. (n = 4−6), $^{**}p<0.01$, $^{***}p<0.001$, considered statistically significant when compared to the control samples.

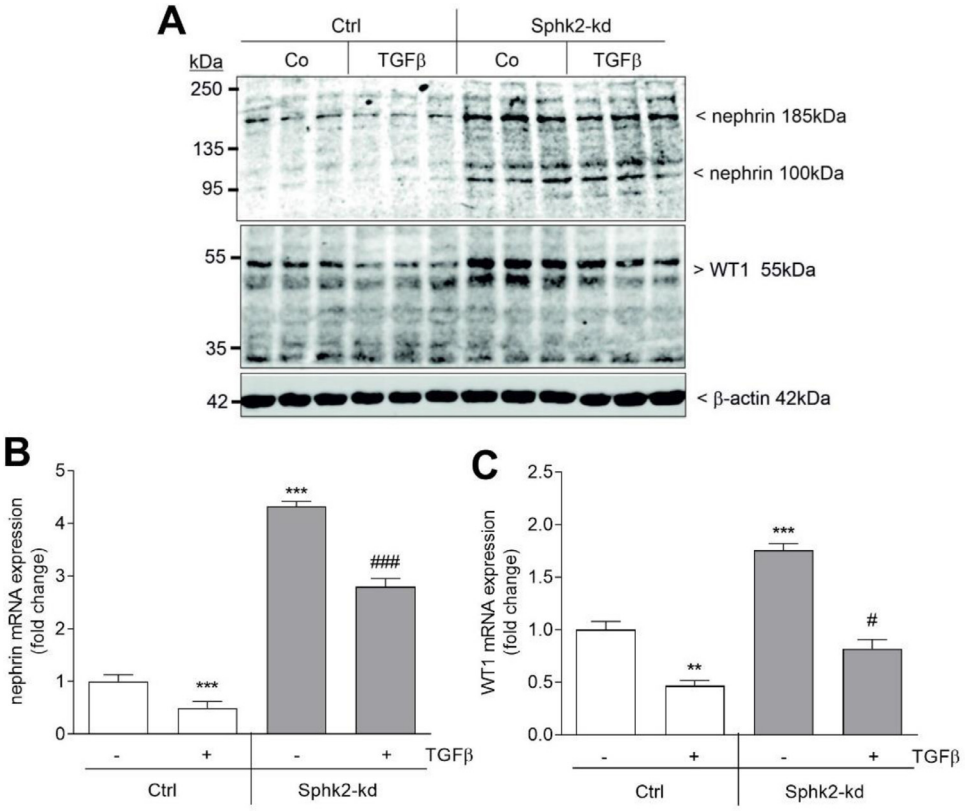

Fig 5. Effect of Sphk2-kd on nephrin and WT1 expression in human podocytes. Human podocytes stably transduced with either a lentiviral control vector (Ctrl) or a Sphk2 shRNA construct (Sphk2-kd) were treated for 24 h with either vehicle (Co, -) or 5 ng/ml of TGFβ_2 (+) and taken for protein extraction, SDS-PAGE and Western blot analysis (A), or RNA extraction and quantitative PCR analysis (B, C) of nephrin and WT1. Bands in A were evaluated by using ImageJ software and data are presented in suppl. Fig. S3. Data in B and C are expressed as fold change compared to controls and are means $\pm$ S.D. ($n = 3$); $^{**}p<0.01$, $^{***}p<0.001$ considered statistically significant when compared to the unstimulated Ctrl values; $^{\#}p<0.05$, $^{\#\#\#}p<0.001$ compared to the unstimulated Sphk2-kd values.

100 kDa [42]. Indeed, a fragment of 100 kDa is often detected in Western blot analysis. However, hypoglycosylated forms and fragments of nephrin are not expected to show functionality at the ultrafiltration barrier. As seen in Fig. 5A, nephrin protein at 185 kDa was markedly increased in Sphk2-kd cells. When cells were stimulated with TGFβ, a key mediator of extracellular matrix (ECM) production and podocytopathy, nephrin protein expression was reduced in both Ctrl and Sphk2-kd cells, but still remained on a higher level in Sphk2-kd cells (Fig 5A, upper panel). WT1 protein expression was regulated in a similar manner by TGFβ and Sphk2-kd as seen for nephrin (Fig. 5A, lower panel). This enhancing effect on nephrin and WT1 protein expression by Sphk2-kd was also observed on the mRNA expression level (Fig. 5B and C) suggesting that a mechanism affecting gene transcription is involved.

To see whether the upregulating effect on nephrin and WT1 by Sphk2-kd is also mimicked by a catalytic Sphk2 inhibitor, we used SLM6031434. Treatment of wildtype podocytes with SLM6031434 for 24 h similarly upregulated nephrin and WT1 protein (Fig. 6A) and mRNA expression (Fig. 6B and C).

Since glomerulosclerosis is a hallmark of diabetic nephropathy, we further investigated whether in human podocytes, fibrotic factors induced by the prototypic fibrotic mediator TGFβ are affected by Sphk2-kd. When podocytes were stimulated with TGFβ, fibrotic markers including connective tissue growth factor (CTGF), fibronectin and plasminogen activator inhibitor 1 (PAI-1) were upregulated on the mRNA expression level (Fig. 7A-C), as well as on the protein level (Fig. 7D). The mRNA and protein expressions of all these factors were diminished by Sphk2-kd (Fig. 7A-D). In addition, we found that the Smad signaling pathway, detected as phosphorylated Smad2, was also reduced by Sphk2-kd (Fig. 7D).

Moreover, treatment of cells with TGFβ in the presence of the Sphk2 inhibitor SLM6031434 also downregulated the mRNA (Fig. 8A-C) and protein expression (Fig. 8D) of CTGF, fibronectin and PAI-1.

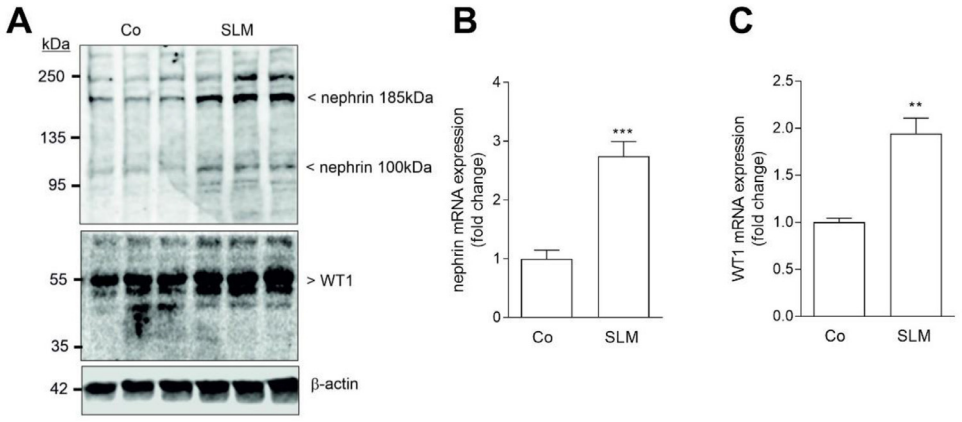

Fig 6. Effect of the specific Sphk2 inhibitor SLM6031434 on nephrin and WT1 expression in human podocytes.
Human wildtype podocytes were treated for 24 h with either vehicle (Co) or the Sphk2 inhibitor SLM6031434 (SLM, 1μM). Thereafter, proteins and RNA were extracted and taken for SDS-PAGE and Western blot analysis of nephrin (A, upper panel), WT1 (A, middle panel) and β-actin (A, lower panel), or RNA extraction and qPCR analysis of nephrin (B) and WT1 (C). For normalization 18S RNA was used. Bands in A were evaluated by using ImageJ software and data are presented in suppl. Fig. S4. Data in B and C are expressed as fold change compared to controls and are means ± *S*.D. ($n = 3$); $^{**}p<0.01$, $^{***}p<0.001$ considered statistically significant when compared to the vehicle-treated control values.

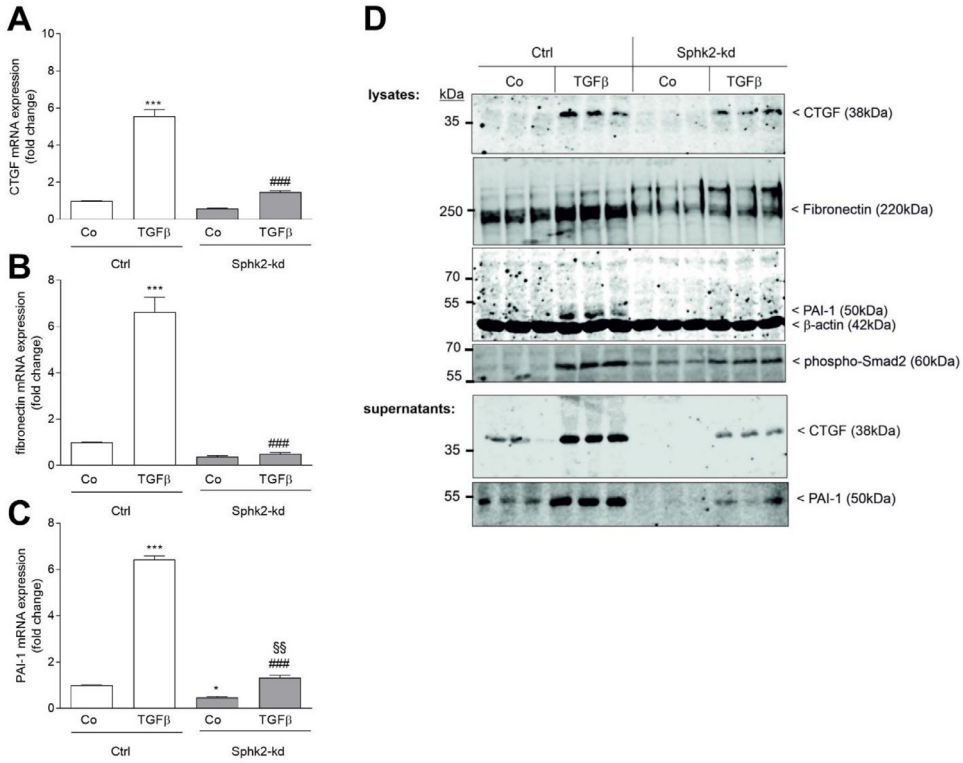

Fig 7. Effect of Sphk2 knockdown on TGFβ-stimulated fibrotic factors in human podocytes. Human podocytes stably transduced with either a lentiviral control vector (Ctrl) or a Sphk2 shRNA construct (Sphk2-kd) were treated for 24 h with either vehicle (Co) or 5 ng/ml of TGFβ_2. Thereafter, RNA was extracted and taken for qPCR analysis of CTGF (A), fibronectin (FN, B), PAI-1 (C) and the house-keeping gene 18S RNA. Data in A-C are expressed as fold change compared to controls and are means ± *S*.D. ($n = 3$); $^{*}p<0.05$, $^{***}p<0.001$ considered statistically significant when compared to the vehicle-treated Ctrl values; $^{\#\#\#}p<0.001$ compared to the TGFβ-treated Ctrl values; $^{\S\S}p<0.01$ compared to the vehicle-treated Sphk2-kd values. (D) Stimulated podocytes were taken for protein extraction (Lysates) or supernatants were taken for protein precipitation by 7% (w/v) trichloroacetic acid. Proteins were then separated by SDS-PAGE, transferred to nitrocellulose and subjected to Western blot analysis of CTGF, fibronectin (FN), PAI-1, phospho-Smad2, and β-actin. A representative Western blot in triplicates is shown in D. Bands were evaluated by using ImageJ software and data are presented in suppl. Fig. S5.

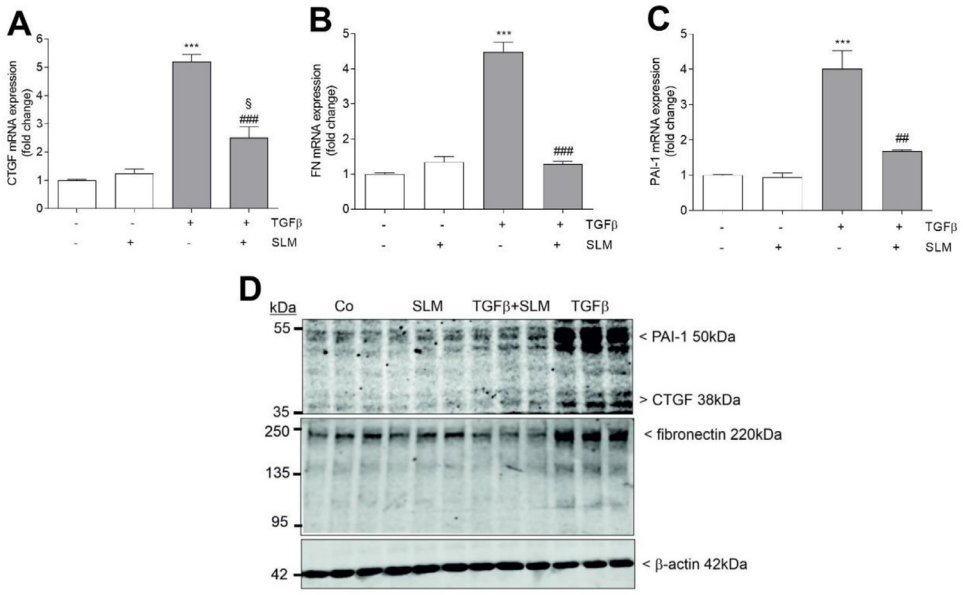

Fig 8. Effect of the Sphk2 inhibitor SLM6031434 on TGFβ-induced fibrotic factors in human podocytes. Wildtype podocytes were treated for 24 h with either vehicle (Co, -), SLM6031434 (SLM, 1μM), TGFβ_2 (5 ng/ml), or TGFβ_2 plus SLM. Thereafter, either RNA or proteins were extracted and taken for quantitative PCR analysis of CTGF (A), fibronectin (FN, B), PAI-1 (C), and 18S RNA, or protein separation by SDS-PAGE, transfer to nitrocellulose and Western blot analysis (D) of CTGF, fibronectin, PAI-1, and β-actin. For data in A-C, ΔΔCt values were calculated according to standard methods. The gene of interest was normalized to 18S RNA, and results are expressed as fold change as compared to controls and are means ± *S*.D. (n = 3); $^{***}p<0.001$ considered statistically significant when compared to the vehicle-treated values; $^{\#\#}p<0.01$, $^{\#\#\#}p<0.001$ compared to the TGFβ-treated values; $^{\S}p<0.05$ compared to the SLM-treated values. Blots in D show one out of three independent experiments performed each in triplicates. Bands were evaluated by using ImageJ software and data are presented in suppl. Fig. S6.

All these data suggest that Sphk2-kd mediates an anti-fibrotic effect.

One of the first line treatment options for many forms of glomerular diseases with increased proteinuria, including glomerulonephritis and nephrotic syndrome, are glucocorticoids. Thus, dexamethasone has been shown to have a direct nephroprotective effect by upregulating nephrin expression [24].

Stimulation of wildtype podocytes with dexamethasone for 24 h, not only upregulated nephrin (Fig. 9B), and WT1 mRNA expressions (Fig. 9C), thus confirming the previous report by Xing et al. (Xing 2006), but also downregulated Sphk2 mRNA expression (Fig. 9A).

The glucocorticoid receptor antagonist RU-486 (mifepristone) reversed the effect of dexamethasone on nephrin, WT1 and Sphk2 (Fig. 9A-C), suggesting that dexamethasone acted through binding to the glucocorticoid receptor. In the same setting, we found that dexamethasone upregulated Sphk1 mRNA expression (suppl Fig. S7A) and downregulated $S1P_1$ (Fig. S7B). $S1P_5$ was slightly increased (Fig. S7E), while the other receptors expressed in podocytes, i.e. $S1P_2$ and $S1P_3$, were not affected (Fig. S7C and D), and $S1P_4$ was not expressed at all. Sphk2 protein was also found to be time-dependently downregulated by dexamethasone (Fig. 9D), and as a consequence of reduced Sphk2, cellular sphingosine increased (Fig. 9E). Notably, Sphk1 protein was only transiently increased by dexamethasone, with a peak at 3−6 h and thereafter returned to basal levels at 24 h. Besides sphingosine, no other sphingolipids were found to be significantly changed after 24 h of dexamethasone treatment (suppl. Fig. S9). Notably, no consistent increase of S1P or dihydro-S1P was seen.

To see whether the sphingosine is the active lipid that affects WT1 upregulation, we stimulated cells with increasing concentrations (up to 10μM) of exogenous sphingosine. This regimen also upregulated WT1 protein (Fig. 9F). In addition, cellular PKC activity was analyzed by staining with a phospho-PKC substrate antibody. Various bands were found to be reduced (Fig. 9F, lower panel) thus confirming previous reports [43], that sphingosine can inhibit at least some of the PKC isoforms expressed in podocytes. We further generated stable knockdown cell lines of the two PKC isoenzymes α and δ, which have previously been reported to regulate renal pathology [34,44]. Strikingly, only when PKCδ was downregulated, WT1 protein expression was increased (Fig. 10), while PKCα knockdown slightly reduced WT1 expression. These data suggest that PKCδ is a likely candidate to negatively regulate WT1

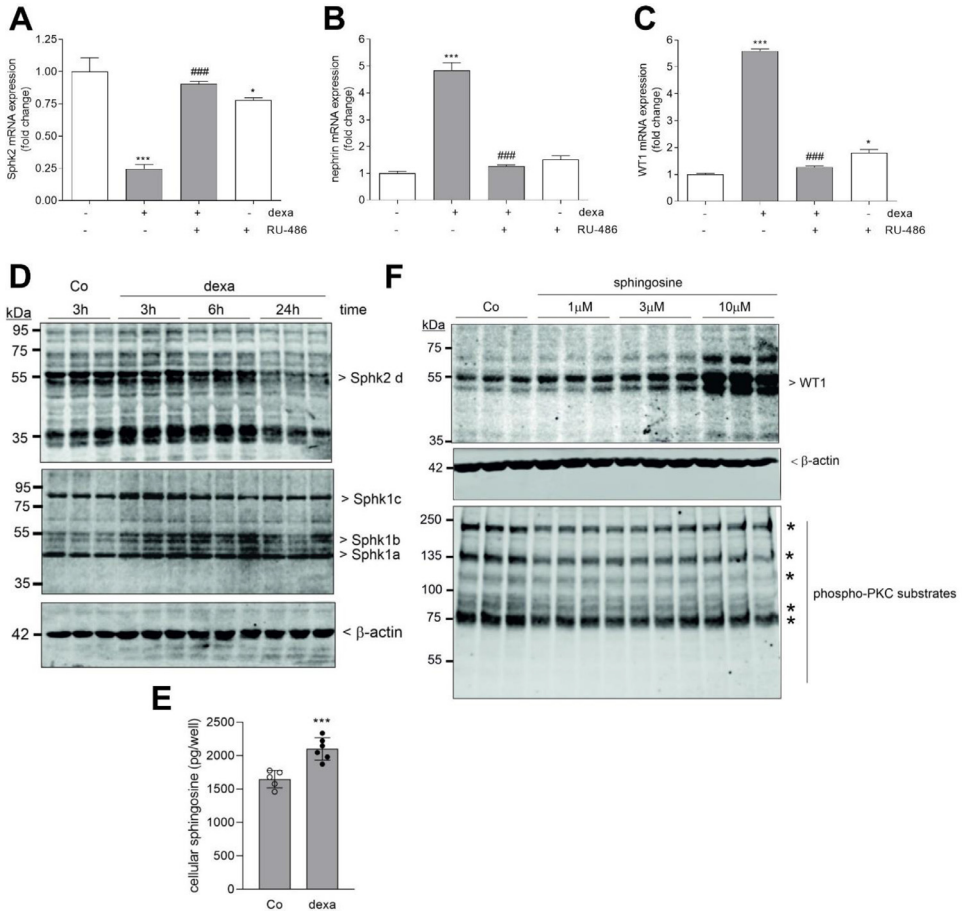

Fig 9. Effect of dexamethasone on Sphk2, nephrin and WT1 mRNA, Sphk2 protein and cellular sphingosine levels in human podocytes. (A-C) Wildtype podocytes were treated for 24 h with either vehicle (-), dexamethasone (dexa, 300 nM), dexa plus RU-486 (10 μM), or RU-486 (10 μM) alone. Thereafter, RNA was extracted and taken for quantitative PCR analysis using primers of Sphk2, nephrin, WT1 and 18S RNA. ΔΔCt values were calculated according to standard methods and normalized to 18S RNA. Data are expressed as fold change as compared to control samples and are means ± *S*.D. ($n = 3$). *$p<0.05$, ***$p<0.001$ considered statistically significant when compared to the control samples; $^{###}p<0.001$ compared to the dexa samples. (D) Podocytes were treated with either vehicle in RPMI (Co, 3 h) or for the indicated time periods with dexamethasone (300 nM). Then, proteins were extracted, separated by SDS-PAGE, transferred to nitrocellulose and taken for Western blot analysis of Sphk2 (upper panel), Sphk1 (middle panel), and β-actin (lower panel). The blot shows one representative experiment performed in triplicated. Bands were evaluated by using ImageJ software and data are presented in suppl. Fig. S8. (E) Podocytes were stimulated for 24 h with either vehicle (Co) or dexamethasone (300 nM). Thereafter, lipid extracts were prepared and sphingosine quantified by LC/MS/MS as described in the methods section. Data are expressed as pg/well and are means +/- S.D. ($n = 5-6$), ***$p<0.001$ compared to control. (F) Podocytes were treated for 24 h with either vehicle (Co) or the indicated concentrations of sphingosine (in μM). Protein extracts were separated by SDS-PAGE, transferred to nitrocellulose and subjected to Western blot analysis using antibodies against WT1 (upper panel), β-actin (middle panel), and phospho-PKC substrate (lower panel). Data show one representative out of two independent experiments performed in triplicates. Bands were evaluated by using ImageJ software and data are presented in suppl. Fig. S10.

expression, and thus, vice versa, PKCδ inhibition or depletion has a protective effect on podocyte function, which is in line with the previous report showing that PKCδ knockout mice were protected from diabetic nephropathy [44].

Finally, we addressed the possible mechanism by which dexamethasone downregulated Sphk2 mRNA expression, which could involve either a suppressive effect on Sphk2 gene transcription or an accelerated decay of Sphk2 mRNA. To this end, cells were pretreated for 30 min with actinomycin D to block de-novo gene transcription, and then treated for different time periods with either medium or dexamethasone. Sphk2 mRNA was followed over time. As seen in Fig. 11A, Sphk2 mRNA decreased much more rapidly in the presence of dexamethasone as compared to controls. The effect of dexamethasone was also concentration dependent, and at 3 h of

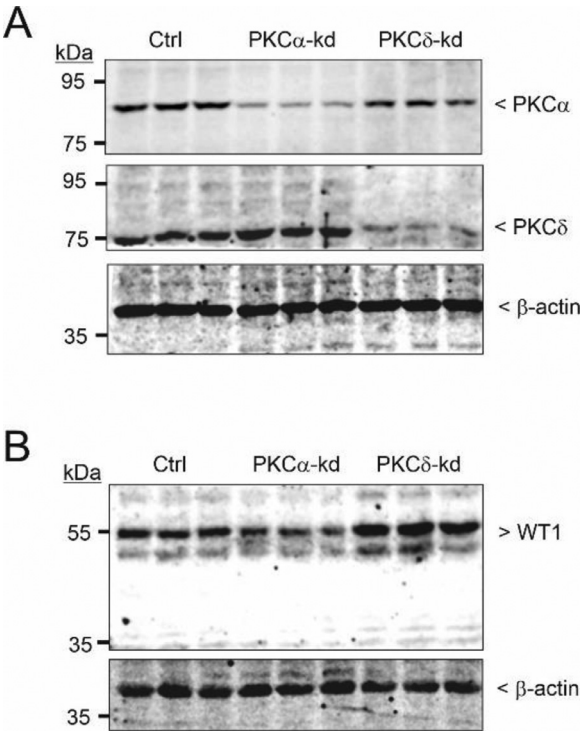

Fig 10. Effect of PKCα and PKCδ knockdown on WT1 protein expression in human podocytes. Human podocytes, transduced with a control construct (Ctrl) or with shRNA constructs of human PKCα (PKCα-kd) or human PKCδ (PKCδ-kd), were incubated for 20 h in serum-free RPMI and taken for protein extraction. Samples were separated by SDS-PAGE, transferred to nitrocellulose and subjected to Western blot analysis of PKCα (A, most upper panel), PKCδ (A, middle panel), WT1 (B, upper panel), or β-actin (A,B, lowest panels). Data show one representative out of two independent experiments performed in triplicates. Bands were evaluated by using ImageJ software and data are presented in suppl. Fig. S11.

incubation with 1 μM of dexamethasone, a 80% reduction of Sphk2 mRNA was apparent (Fig. 11B). These data suggest that dexamethasone acts by altering Sphk2 mRNA stability.

Discussion

This study shows for the first time that Sphk2 has a key function in glomerular podocytes by regulating the transcription factor WT1 and its target gene nephrin. Loss of Sphk2 expression, or its catalytic inhibition, leads to an upregulation of WT1 and nephrin expression, which mediates a protection to podocytes and the ultrafiltration barrier, and consequently prevents protein loss into the urine.

We suggest here that the mechanism for this protective effect of Sphk2 downregulation involves sphingosine accumulation that leads to PKCδ inhibition, which in turn, enhances WT1 expression, and finally triggers enhanced nephrin gene transcription and protein synthesis.

WT1 is a key transcription factor that regulates multiple target genes in the kidney. By genome-wide analysis of the WT1 transcriptional network in podocytes, it was previously shown that WT1 regulates many of the identified genes, that, when mutated, cause podocytopathy and a nephrotic syndrome [45]. In addition, genetic mutations in the WT1 gene couple to a nephrotic syndrome and various forms of glomerulosclerosis that ultimately progress to renal failure [46].

WT1 is a protein with multiple (at least 14) transcript variants that result from alternative splicing at two coding exons [47]. In Fig. 3A homogenates of entire mouse renal cortex were used for Western blot analysis. All protein bands with a range from 50 to 75 kDa resulting from the WT1 alternative splicing are quantified densitometrically. As renal cortex consists of various cell types it is conceivable that the protein pattern of WT1 in Fig. 3A differs from those expressed by human podocytes (Fig. 5 and Fig. 6).

WT1 can either activate or suppress gene transcription. Thus, genes like nephrin [37,48] and podocalyxin [49] are transcriptionally activated by WT1, while the fibrotic mediator TGFβ1 is rather suppressed by WT1 [50]. Transcriptional activity of WT1 is also regulated by phosphorylation. In this view, it was reported that PKC and PKA can both phosphorylate WT1 in vitro, and phosphorylation by these kinases inhibits the ability of WT1 to bind cognate DNA elements [51]. So, if activation of PKC inhibits WT1, as shown by these authors, then, one could also hypothesize that inhibition of PKC may promote WT1 transcriptional activity. In fact, sphingosine, which accumulates upon Sphk2 downregulation (Fig. 4C), is well known as an endogenous PKC inhibitor with an IC_{50} of 1−6 μM [43,52]. Our data are in agreement with such a mechanism as we could show that in podocytes, sphingosine indeed reduces cellular PKC activity and enhances WT1 protein expression (Fig. 9F). The influence of PKC in podocytes is still little understood and this may be due to the complex nature of PKC existing as a family of 11 isoforms with probably differential functions. Notably, it was shown that PKC-α knockout mice are protected from diabetic nephropathy and interestingly, are also protected from a loss of nephrin expression [34]. PKC-α was also identified as an important mediator of nephrin endocytosis, which vice versa suggests, that inhibition of PKC-α should prevent nephrin endocytosis and degradation [53]. Similarly, PKCδ knockout mice are also protected from diabetic nephropathy [44]. Our data, using both PKCα and PKCδ knockdown cells, rather point to PKCδ as the enzyme involved in WT1 regulation (Fig. 10B). PKCδ has previously been appointed a key role as pro-apoptotic enzyme [54], and thus, vice versa, an inhibition of PKCδ should enhance

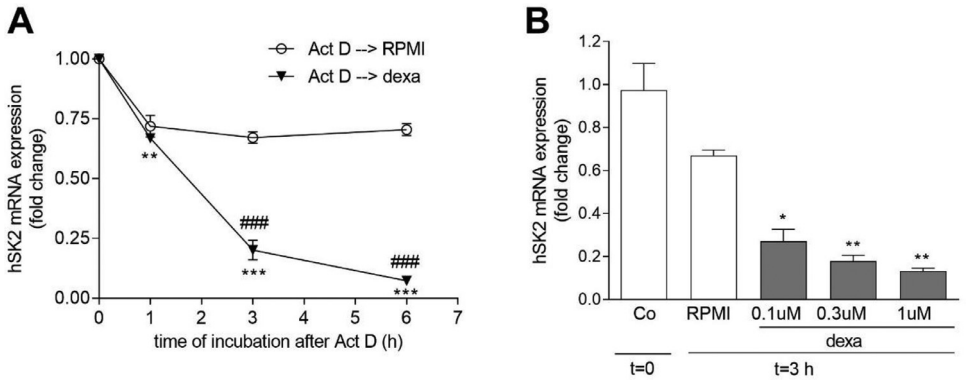

Fig 11. Effect of dexamethasone on Sphk2 mRNA degradation in human podocytes. (A) Human wildtype podocytes were pretreated for 30 min with actinomycin D (Act D, 10 μM) and then treated with either RPMI (open circles) or dexamethasone (300 nM, closed triangles) up to 6 h. (B) Podocytes were pretreated for 30 min with actinomycin D (10 μM, $t = 0$) and then stimulated for 3 h ($t = 3$ h) with either RPMI or the indicated concentrations of dexamethasone (dexa). RNA was extracted from cells and taken for quantitative PCR analysis using primers of Sphk2 and 18S RNA. ΔΔCt values were calculated according to standard methods. Sphk2 expression was normalized to 18S RNA, and results are expressed as fold change as compared to controls and are means ± S.D. ($n = 3$); in A: $^{**}p<0.01$, $^{***}p<0.001$ considered statistically significant when compared to the time 0 sample; $^{###}p<0.001$ compared to the corresponding RPMI-treated samples; in B: $^{*}p<0.05$, $^{**}p<0.01$, compared to the control RPMI-treated samples.

survival of cells. Whether such a mechanism also occurs in podocytes is still unknown.

Most importantly, our data confirm that nephrin is a key regulator of the glomerular ultrafiltration barrier. Ample evidence has been accumulated over the years showing that reduced expression of nephrin is coupled to podocyte foot process effacement, loss of glomerular barrier integrity and proteinuria, while on the opposite, an increased nephrin expression rather stabilizes foot processes and mediates protection. This has emerged from genetic studies showing that mutations in the nephrin gene cause various forms of nephrotic syndromes, including the congenital nephrotic syndrome of the Finnish type [55,56]. Furthermore, in many forms of nephrotic syndromes and glomerular diseases, nephrin is downregulated [57]. On the molecular level, factors that downregulate nephrin expression are all known to cause podocytopathy and participate in the pathogenesis of glomerular disease. These factors include angiotensin II [58] and VEGF [59], but also the inflammatory cytokines interleukin-1β and tumor necrosis factor-α [60].

Mechanistically, there are at least three different ways to downregulate nephrin protein expression in the slit diaphragm: (1) by shedding of nephrin protein from the cell surface by proteases and subsequent urinary excretion, (2) accelerated internalization of nephrin followed by degradation [61], and (3) reduced nephrin gene transcription and protein de-novo synthesis [58]. Accordingly, increased nephrin levels can be obtained by reduced shedding, reduced endocytosis or by enhanced gene transcription. Our study on Sphk2 knockout and catalytic inhibition favours the mechanism of enhanced gene transcription. This is stressed by the findings that loss of Sphk2 involves an increased nephrin mRNA and protein expression (Fig. 5B), as well as an increased expression of the transcription factor WT1 that is key for nephrin transcription.

Our data also show that the glucocorticoid dexamethasone, which has been appointed a direct protective effect on glomerular cells [23,24,62] exceeding the suppressive effect on immune cells [63], and is still one of the first line medications to treat a nephrotic syndrome, acts at least partially through downregulating Sphk2 protein expression (Fig. 9D) and consequently increasing cellular sphingosine levels (Fig. 9E) and consequently WT1 mRNA expression (Fig. 9C). We propose that the mechanism involves dexamethasone-induced Sphk2 mRNA decay (Fig. 11) and reduced protein expression. Generally, mRNA degradation can be stimulated either by increased binding of RNA destabilization factors, such as tristetraprolin or others [64], or by reduced binding of RNA stabilization factors such as the embryonic lethal abnormal vision (ELAV) protein family including HuR [65]. Which mechanism finally holds true for the degradation of Sphk2 still needs to be determined.

Previously, the role of Sphk2 was also addressed in lupus nephritis, another glomerular disease model [66,67]. In the mouse strain MRL/MpJ-Faslpr/2 J (MRL/lpr), which spontaneously develops lupus nephritis, Snider et al. reported that the Sphk2 inhibitors ABC294640 only had minor effects on glomerular injury and interstitial abnormalities, which were only seen by trend but failed to show a statistical significance. No effect on albuminuria was detected in that model [66]. However, it should be noted that ABC294640 is a relatively weak Sphk2 inhibitor showing an IC_{50} value of 60 μM in vitro [68]. In another model of pristane-induced lupus nephritis,

Sphk2-deficient mice showed no improvement over control mice in terms of total proteinuria. In contrast to these glomerular models, that failed to detect a beneficial effect of Sphk2 depletion or inhibition, various interstitial nephritis models could clearly document a marked disease reduction by loss of Sphk2 [27-29]. Since the interstitial cells, that participate in interstital nephritis and fibrosis, do not express nephrin, the mechanism is clearly different than the one proposed in our diabetic nephropathy model. In this view, Bajwa et al. proposed an enhanced interferon-γ production as the key anti-fibrotic mechanism [27], while Schwalm et al. suggested the upregulation of Smad7 as a key mechanism [28]. Furthermore, Ghosh et al. showed that Sphk2 depletion or inhibition causes a switch in macrophage polarization towards the anti-inflammatory M2 macrophages [29].

In summary, our data demonstrate for the first time, that Sphk2 has a key function in glomerular podocytes by regulating the transcription factor WT1 and its target gene nephrin (Fig. 12). Downregulation of Sphk2, or pharmacological inhibition, enhances nephrin expression and mediates a nephroprotective effect. This suggests that Sphk2 indeed represents a novel attractive pharmacological target to stabilize podocyte foot processes and thereby to reduce proteinuria in kidney diseases.

Experimental procedures

Chemicals and reagents

Human transforming growth factor (TGF) β_2 was from Peprotech (London, UK); 2-deoxy-2-({[*methyl*(*nitroso*)*amino*]carbonyl}amino)-β-D-glucopyranose (streptozotocin, STZ), dimethyl sulfoxide (DMSO), dexamethasone, RU-486 (mifepristone), actinomycin D, puromycin, glycerol stocks of hSphk2-specific shRNA sequences in pLKO.1-puro vector (MISSION® shRNA), KAPA SYBR® FAST qPCR mix, RPMI 1640, horse serum, fatty acid-free BSA and bovine insulin were from Sigma Aldrich Chemie GmbH (Buchs, Switzerland). SLM6031434/HCl was from Tocris Bioscience (Bristol, UK); sphingosine was from Cayman Chemicals/Adipogen AG, Liestal, Switzerland; fluorescently labelled Odyssee IRDye® 800CW goat anti-mouse or anti-rabbit IgG secondary antibodies were from LI-COR Biosciences (Bad Homburg, Germany). Primers for qPCR were from Eurofins Genomics Germany GmbH (Ebersberg, Germany). The First Strand DNA Synthesis Kit was from ThermoFisher Scientific (Zug, Switzerland); RNAsolv® was from VWR International AG (Dietikon, Switzerland). Fetal bovine serum (FBS) was from PAN-Biotech GmbH (cat.no P40−37,

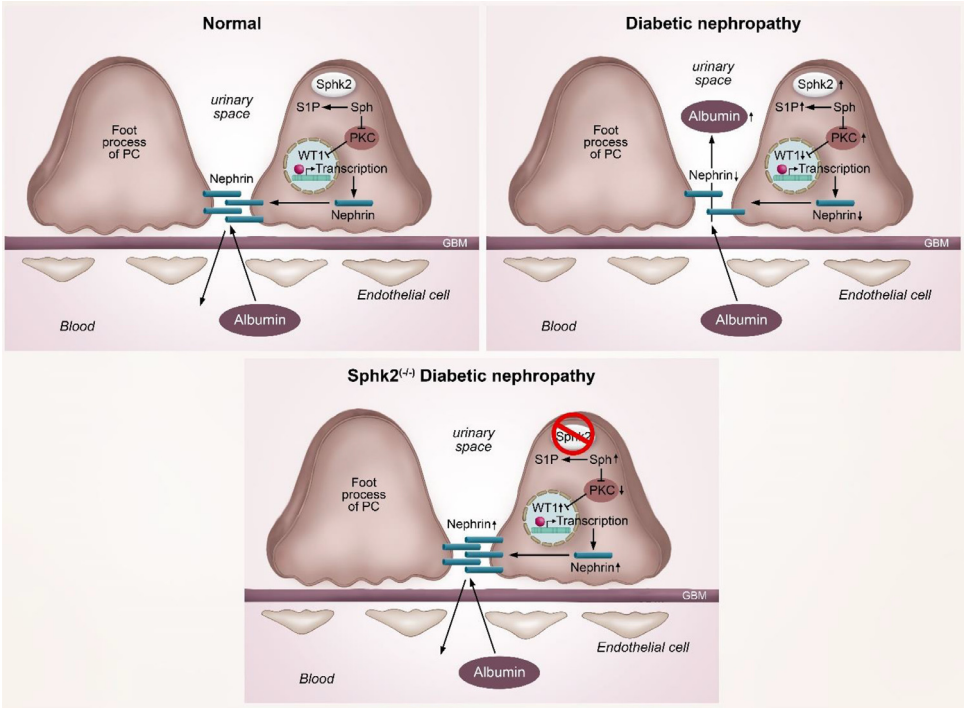

Fig 12. Schematic presentation of the podocyte slit diaphragm and the possible mechanism of regulation by Sphk2 depletion. View on the podocyte slit diaphragm that is built by interactions of proteins of neighbouring foot processes including nephrin under normal healthy conditions (upper left panel), diabetic nephropathy (upper right panel), and Sphk2 depleted diabetic nephropathy (lower panel). For clarity reasons, only the here investigated factors are depicted. Abbreviations: PC, podocyte; PKC, protein kinase C; GBM, glomerular basement membrane; S1P, sphingosine 1-phosphate; Sph, sphingosine; Sphk2, sphingosine kinase 2; WT1, Wilm's tumor suppressor gene 1.

Aidenbach, Germany). All other cell culture nutrients were from Life Technologies AG (Basel, Switzerland).

Commercial antibodies were as follows: β-actin (clone AC-15 from Sigma Aldrich Chemie GmbH, Buchs, Switzerland); α-tubulin (cat.no T9026, Sigma Aldrich Fine Chemicals); phospho-(S^{465}/S^{467}) Smad2 (cat.no. 3108; Cell Signaling/Bioconcept, Allschwil, Switzerland); phospho-PKC substrate (cat.no 2261, Cell Signaling/Bioconcept, Allschwil, Switzerland); nephrin (for IHC use: ab227806 from Abcam; for Western blot use: Eurogentec S.A., see below), WT-1 (for IHC and Western blot use: ab242425 from Abcam; for Western blot use: C-19 from Santa Cruz Biotechnology, Heidelberg, Germany); CTGF antibody (E-5 from Santa Cruz Biotechnology; fibronectin (ab2413 from Abcam), PAI-1 (H-135 from Santa Cruz Biotechnology).

Peptide synthesis and polyclonal antibody generation

Peptide synthesis and anti-hSphk2 antiserum generation was performed by Eurogentec S.A. (Seraing, Belgium) as previously described [28]. Briefly, two synthetic peptides, NGHLEAEEQQDQRPD and CLPGDGEITPDLLPRP based on the N-terminal sequence of human sphingosine kinase-2 (accession number: NM_020126), were synthesized and coupled to keyhole-limpet hemocyanin, and used to immunize rabbits. The terminal serum (no.SA2866) was taken for Western blot analyses. The human Sphk1 antibody (Ab-64) was generated and characterized as described in a previous study [69].

A nephrin antibody was generated as previously described [70] based on the two peptides (CEYEESQWTGERDTQS and QPSGEPEDQLPTEPPC) of rat nephrin, which are identical to the human sequence. The antibody (SA-1515) was previously characterized to recognize human nephrin in Western blot analyses [71]. We further validated the antibody by transfection of podocytes with siRNA of human nephrin (siNPHS1) (sc-36,030, Santa Cruz Biotechnology, Heidelberg, Germany) to confirm that bands at 185 and 100 kDa represent nephrin (suppl. Fig. S12).

Polyclonal antibodies against PKCα and PKCδ were kindly provided by Dr. Doriano Fabbro (Basel).

Cell culturing and stable Sphk2 knockdown generation

Immortalized human podocytes were isolated and immortalized according to previous reports [72,73] and cultivated in RPMI medium supplemented with 10% (vol/vol) FBS, 10 mM Hepes, pH 7.4, 1% (vol/vol) non-essential amino acid solution, 6 μg/ml bovine insulin, 5 μg/ml transferrin, 5 nM sodium selenite, 100 units/ml penicillin and 100 μg/ml streptomycin. Cells were cultured at 33 °C under 5% CO_2 atmosphere. At 80−90% confluency, the culturing temperature was changed to 37 °C to allow differentiation of podocytes. Prior to stimulation, cells were incubated for 2−4 h in RPMI medium containing 10 mM Hepes, pH 7.4 and 0.1 mg/ml fatty acid-free bovine serum albumin (BSA) as indicated in the figure legends.

Stable knockdown of Sphk2 in hPC was achieved by transduction of cells at 33 °C with five different lentiviral short hairpin RNA (shRNA) constructs from Sigma MISSION® (TRCN0000036969, TRCN0000036970, TRCN0000036971, TRCN0000036972, TRCN0000036973; all in pLKO.1-puro vector) following the manufacturer's protocol. Virus control cells were generated with TRC2 pLKO.5-puro empty vector control plasmid DNA from the same company. For selection of resistant colonies 1 μg/ml of puromycin was added to the medium. Knockdown efficiency was confirmed by quantitative PCR for mRNA expression, and by Western blot analysis for protein expression. Best knockdown was obtained with TRCN0000036970. These cells were named hPC-Sphk2-kd and taken for further experiments. Stable knockdown of PKCα and PKCδ were generated by the same procedure using 5 different shRNA constructs for each enzyme. Best knockdown was obtain with TRCN0000196730 (for PKCα, further denoted PKCα-kd) and TRCN0000195408 (for PKCδ, further denoted PKCδ-kd).

Streptozotocin (STZ)-induced diabetes mellitus in mice

Diabetes mellitus was induced in 8-week-old wild-type C57BL/6 J (WT) and *Sphk2*$^{-/-}$ mice (Sphk2^{tm1geno}; generated by GenOway S.A., Lyon (France), and backcrossed to C57BL/6 J) by five consecutive daily intraperitoneal injections of STZ at a dose of 50 mg/kg body weight, dissolved in 100 mmol/L sodium citrate buffer (pH 4.5). Mice were fasted for at least 6 h prior to each injection. Blood glucose was measured by tail vein sampling (Accu-Check, Roche Diagnostics GmbH, Mannheim, Germany) two weeks after the last STZ injection.

Approximately 80% of mice injected with STZ developed a morning blood glucose level of >16 mM (288 mg/dL) and were included in the experiment as diabetic animals. WT and *Sphk2*$^{-/-}$ mice injected only with sodium citrate buffer were used as controls. Mice that developed glucosuria (50%) received a subcutaneous insulin implant (Linplant®) (Linshin, Ontario, Canada) to prevent ketoacidosis. Equal number of mice treated with insulin pallets per genotype (n = 3) was included in the experiment.

Blood glucose levels were controlled every 10 days (Haemo-Glukotest; Roche Diagnostics, Mannheim, Germany). Urinary glucose and ketones were measured with reagent strips (Keto-Diastix Reagent Strips, Bayer Vital, Leverkusen, Germany). Albuminuria was quantified using the mouse Albumin ELISA kit (Exocell, Philadelphia, PA, USA). Urinary creatinine excretion was determined using the Colorimetric Microplate Assay (Oxford Biomedical Research, Rochester Hill, MI, USA). Kidneys (n = 6 per group) were harvested and analyzed 60 days after induction of diabetes. All procedures were conducted in accordance with the German Animal Protection Act and were approved by the Ethics Review Committee for laboratory animals of the District Government of Darmstadt, Germany.

Immunohistochemistry

The 3 μm sections of paraformaldehyde-fixed, paraffin-embedded kidney samples were deparaffinized with xylene and then rehydrated. Antigen retrieval was performed in Dako EDTA buffer pH 9.0 (DAKO GmbH Germany) by 10 min microwave treatment. Endogenous peroxidase activity was quenched with 3% hydrogen peroxidase at room temperature for 10 min. Tissue sections were blocked with Blocking/Protein Block Dako (DAKO GmbH Germany) for 20 min followed by overnight incubation at 4 °C with anti-nephrin (Abcam, ab227806), anti-WT1 (Abcam, ab242425), or rat-anti-mouse-F4/80 (Bio-Rad, MCA497G) antibodies for the macrophage detection (anti-nephrin antibody diluted 1:1000, anti-WT1 antibody 1:100, anti-F4/80 antibody 1:250) in Background Reducing Components (DAKO GmbH Germany). Subsequent to washing steps, renal sections were developed with Simple Stain MAX PO Universal Immuno-Peroxidase Polymer Histofine MaxPo anti-Rabbit (Nichirei Biosceinces INC, Tokyo, Japan) and visualized using diaminobenzidine substrate (DAKO GmbH Germany). The tissues were counterstained with Harris hematoxylin. Microscopic observations were carried out with a standard Olympus BX60 light microscope. The density of nephrin-positive staining was quantified with free software ImageJ Fiji. The number of F4/80$^+$ was estimated per high-power field (HPF 400×, with a minimum of 10 fields counted). Histological examinations were performed by two observers blinded to the conditions.

Western blot analysis

Stimulated cells were washed with ice-cold phosphate-buffered saline (PBS) and subsequently scraped into lysis buffer (50 mM Tris/HCl pH 7.4, 150 mM sodium chloride, 10% (v/v) glycerol, 1% (v/v) Triton X100, 2 mM EDTA, 2 mM EGTA, 40 mM β-glycerol phosphate, 50 mM sodium fluorid, 10 mM sodium pyrophosphate, 2 mM dithiotreitol, 200 μM sodium orthovanadate, 400 μl reconstituted complete™ protease inhibitor cocktail). Cells were homogenized by a sonicator for 10 s and lysates were centrifuged for 10 min at 14′000 x g. Supernatants were taken for protein determination. Equal amounts of protein (80 μg per lane) in Laemmli buffer were separated by SDS-PAGE, transferred to a nitrocellulose membrane (for nephrin and fibronectin, 0.03% (w/vol) SDS was added to the transfer buffer) and subjected to Western blot analysis according to standard protocols. As secondary antibodies, IRDye® IgGs were used, and membranes were wet-scanned with a LI-COR Odyssey® CLx imaging system using 700 nm and 800 nm channels for multi-color analysis, visualized using ImageStudio software version 5.2 (LICOR Biosciences). For processing of kidney samples, the renal cortex was homogenized, and 40 μg of the homogenate was separated on 8% SDS-PAGE and transferred to nitrocellulose membrane. After blocking with Roti-Block solution (Carl Roth GmbH), the membrane was respectively blotted with purified rabbit monoclonal antibodies against nephrin (Abcam, ab227806) or Wilm's tumor suppressor gene 1 (WT1) (Abcam, ab242425), followed by HRP-conjugated anti-rabbit IgG (GE Healthcare, NA934V). The images were detected by enhanced chemiluminescence detection reagents (Thermo scientific).

RNA extraction and quantitative PCR analysis

Stimulated cells were washed with ice-cold PBS and homogenized in RNA-Solv® reagent. Total RNA extraction was performed according to instructions of the manufacturer. Yield and purity of the isolates were assessed with NanoDrop® ND-1000 spectrophotometer (Witec AG, Littau, Switzerland), and first strand cDNA was synthesized using 1 μg total RNA as template. SYBR® Green based quantitative PCR was performed in a BioRad CFX Connect™ Optics Module thermal cycler (Bio-Rad Laboratories Inc., Hercules, USA) The Bio-Rad CFX Manager software was used to monitor the melting curve, and to obtain the quantification data. The relative mRNA expression of the gene of interest was calculated with the ΔΔCt method normalized to 18S RNA as a housekeeping gene. Primers used were as follows: hSph2: forward: 5′-tcaacctcaagacagaacgac-3′; reverse: 5′-catcccactcactcagcctcag-3′. hPAI-1: forward: 5′-acaaggacgagatcagcaccac-3′; reverse: 5′-tgtgtgtcttcacccagtcattg-3′. hCTGF: forward: 5′-tgcctgccattacaactgtcc-3′; reverse: 5′-gccatgtctccgtacatcttcc-3′. Human fibronectin: forward: 5′-ctgcgagagacctgaag-3′; reverse: 5′-ccaatcttgtaggactgacc-3′. hWT1: forward: 5′-ataaccacacaacgcccatc-3′; reverse: 5′-tcagatgccgaccgtacaag-3′. Human nephrin: forward: 5′-gaggaccgagtcaggaacga-3′; reverse: 5′-tcacctgtgaaacctcggga-3′.

Quantification of S1P and sphingosine by LC-MS/MS

Cell monolayers in 35 mm-diameter dishes were trypsinized, pelleted and resuspended in methanol containing C17-sphingosine, C17-S1P, C17-dihydro-sphingosine, and C17-dihydro-S1P as internal standards, and were subjected to lipid extraction and LC-MS/MS analysis, as previously described [74].

Statistical analysis

Statistical analysis was performed by one-way ANOVA without matching or unpaired *t*-test where applicable. For multiple comparisons the level of significance was calculated with Bonferroni correction. GraphPad Prism 6 Software (La Jolla, CA, USA) was used for statistical analysis and graph representations.

Declaration of Competing Interest

None.

Acknowledgments

This work was supported by the Swiss National Science Foundation (310030_175561/1, to AH), the German Research Council (SFB 815, project A5; SFB 1039, project-ID: 204083920 (to JP and LS); SFB 1177, project-ID: 259130777-E02 and the Cardio-Pulmonary Institute (CPI), EXC 2026, Project ID: 390649896 (all to LS), and the Hochschulstiftung der Universität Bern (to FI). We thank the Department of Clinical Pharmacology, University Hospital Frankfurt am Main, for help and assistance with the LC/MS analysis of sphingolipids.

Supplementary materials

Supplementary material associated with this article can be found in the online version at doi:10.1016/j.matbio.2021.05.003.

Received 26 January 2021;
Received in revised form 10 May 2021;
Accepted 10 May 2021
Available online 17 May 2021

Keywords:
Sphk2;
S1P;
Nephrin;
Wilm's tumor suppressor 1;
Podocytes;
Glomerular disease;
Diabetic nephropathy

Abbreviations:
BSA, bovine serum albumin; CTGF, connective tissue growth factor; DMSO, dimethyl sulfoxide; ECM, extracellular matrix; FBS, fetal bovine serum; FN, fibronectin; kd, knockdown; LC-MS/MS, liquid chromatography−mass spectrometry; PBS, phosphate-buffered saline; PAI-1, plasminogen activator inhibitor 1; PKC, protein kinase C; RU-486, mifepristone; SDS-PAGE, sodium dodecyl sulfate polyacrylamide gel electrophoresis; Sphk, sphingosine kinase; S1P, sphingosine 1-phosphate; STZ, streptozotocin; TGFβ, transforming growth factor β; WT1, Wilm's tumor suppressor gene 1

References

[1] A. Huwiler, J. Pfeilschifter, Sphingolipid signaling in renal fibrosis, Matrix Biol. 68-69 (2018) 230–247.
[2] B. Stepanovska, A. Huwiler, Targeting the S1P receptor signaling pathways as a promising approach for treatment of autoimmune and inflammatory diseases, Pharmacol. Res. (2019).
[3] S. Pyne, D.R. Adams, N.J. Pyne, Sphingosine 1-phosphate and sphingosine kinases in health and disease: recent advances, Prog. Lipid Res. 62 (2016) 93–106.
[4] Y. Kihara, Lysophospholipid receptor nomenclature review: IUPHAR review 8, Br. J. Pharmacol. 171 (15) (2014) 3575–3594.
[5] V.A. Blaho, T. Hla, An update on the biology of sphingosine 1-phosphate receptors, J. Lipid Res. 55 (8) (2014) 1596 -608.
[6] R.L. Proia, T. Hla, Emerging biology of sphingosine-1-phosphate: its role in pathogenesis and therapy, J. Clin. Invest. 125 (4) (2015) 1379–1387.
[7] R. Alemany, Regulation and functional roles of sphingosine kinases, Naunyn Schmiedebergs Arch. Pharmacol. 374 (5−6) (2007) 413–428.
[8] A. Huwiler, J. Pfeilschifter, New players on the center stage: sphingosine 1-phosphate and its receptors as drug targets, Biochem. Pharmacol. 75 (10) (2008) 1893 -900.
[9] D. Hatoum, Mammalian sphingosine kinase (SphK) isoenzymes and isoform expression: challenges for SphK as an oncotarget, Oncotarget 8 (22) (2017) 36898–36929.
[10] J.D. Saba, Fifty years of lyase and a moment of truth: sphingosine phosphate lyase from discovery to disease, J. Lipid Res. 60 (3) (2019) 456–463.
[11] N. Haddadi, "Dicing and splicing" sphingosine kinase and relevance to cancer, Int. J. Mol. Sci. 18 (2017) (9).
[12] M.L. Allende, Mice deficient in sphingosine kinase 1 are rendered lymphopenic by FTY720, J. Biol. Chem. 279 (50) (2004) 52487-52492.
[13] Y. Kharel, Sphingosine kinase 2 is required for modulation of lymphocyte traffic by FTY720, J. Biol. Chem. 280 (44) (2005) 36865-36872.
[14] S. Pyne, Role of sphingosine kinases and lipid phosphate phosphatases in regulating spatial sphingosine 1-phosphate

signalling in health and disease, Cell. Signal. 21 (1) (2009) 14–21.
[15] K. Mizugishi, Essential role for sphingosine kinases in neural and vascular development, Mol. Cell. Biol. 25 (24) (2005) 11113-21.
[16] B. Zemann, Sphingosine kinase type 2 is essential for lymphopenia induced by the immunomodulatory drug FTY720, Blood 107 (4) (2006) 1454–1458.
[17] Y. Kharel, Mechanism of sphingosine 1-phosphate clearance from blood, Biochem. J. 477 (5) (2020) 925–935.
[18] H. Pavenstadt, W. Kriz, M. Kretzler, Cell biology of the glomerular podocyte, Physiol. Rev. 83 (1) (2003) 253–307.
[19] W. Kriz, Podocyte is the major culprit accounting for the progression of chronic renal disease, Microsc. Res. Tech. 57 (4) (2002) 189–195.
[20] W. Kriz, The podocyte's response to stress: the enigma of foot process effacement, Am. J. Physiol. -Renal Physiol. 304 (4) (2013) F333–F347.
[21] T.G. Lopes, Markers of renal fibrosis: how do they correlate with podocyte damage in glomerular diseases? PLoS ONE 14 (2019) (6).
[22] M.J. Randles, Basement membrane ligands initiate distinct signalling networks to direct cell shape, Matrix Biol. 90 (2020) 61–78.
[23] J.E. Goodwin, Role of the glucocorticoid receptor in glomerular disease, Am. J. Physiol. -Renal Physiol. 317 (1) (2019) F133–F136.
[24] C.Y. Xing, Direct effects of dexamethasone on human podocytes, Kidney Int. 70 (6) (2006) 1038–1045.
[25] M. AlQudah, T.M. Hale, M.P. Czubryt, Targeting the renin-angiotensin-aldosterone system in fibrosis, Matrix Biol. (2020) 92–108 91-92.
[26] M. Allinovi, Anti-fibrotic treatments: a review of clinical evidence, Matrix Biol. (2018) 333–354 68-69.
[27] A. Bajwa, Sphingosine kinase 2 deficiency attenuates kidney fibrosis via IFN-gamma, J. Am. Soc. Nephrol. 28 (4) (2017) 1145–1161.
[28] S. Schwalm, Sphingosine kinase-2 deficiency ameliorates kidney fibrosis by up-regulating smad7 in a mouse model of unilateral ureteral obstruction, Am. J. Pathol. 187 (11) (2017) 2413–2429.
[29] M. Ghosh, Cell-intrinsic sphingosine kinase 2 promotes macrophage polarization and renal inflammation in response to unilateral ureteral obstruction, PLoS ONE 13 (2018) (3).
[30] C.O. Eleazu, Review of the mechanism of cell death resulting from streptozotocin challenge in experimental animals, its practical use and potential risk to humans, J. Diabetes Metab. Disord. 12 (1) (2013) 60.
[31] S. Menini, Increased glomerular cell (podocyte) apoptosis in rats with streptozotocin-induced diabetes mellitus: role in the development of diabetic glomerular disease, Diabetologia 50 (12) (2007) 2591–2599.
[32] H. Ahola, Cloning and expression of the rat nephrin homolog, Am. J. Pathol. 155 (3) (1999) 907–913.
[33] A. Benigni, Selective impairment of gene expression and assembly of nephrin in human diabetic nephropathy, Kidney Int. 65 (6) (2004) 2193–2200.
[34] J. Menne, Nephrin loss in experimental diabetic nephropathy is prevented by deletion of protein kinase C alpha signaling in-vivo, Kidney Int. 70 (8) (2006) 1456–1462.
[35] F.N. Ziyadeh, G. Wolf, Pathogenesis of the podocytopathy and proteinuria in diabetic glomerulopathy, Curr. Diabetes Rev. 4 (1) (2008) 39–45.
[36] K.D. Wagner, N. Wagner, A. Schedl, The complex life of WT1, J. Cell Sci. 116 (9) (2003) 1653–1658.
[37] N. Wagner, The major podocyte protein nephrin is transcriptionally activated by the Wilms' tumor suppress or WT1, J. Am. Soc. Nephrol. 15 (12) (2004) 3044–3051.
[38] H. Liu, Molecular cloning and functional characterization of a novel mammalian sphingosine kinase type 2 isoform, J. Biol. Chem. 275 (26) (2000) 19513-19520.
[39] N. Haddadi, “Dicing and splicing” sphingosine kinase and relevance to cancer, Int. J. Mol. Sci. 18 (2017) (9).
[40] H.A. Neubauer, S.M. Pitson, Roles, regulation and inhibitors of sphingosine kinase 2, FEBS J. 280 (21) (2013) 5317–5336.
[41] Y. Kharel, Sphingosine kinase 2 inhibition and blood sphingosine 1-phosphate levels, J. Pharmacol. Exp. Ther. 355 (1) (2015) 23–31.
[42] M.M. Rinschen, N-degradomic analysis reveals a proteolytic network processing the podocyte cytoskeleton, J. Am. Soc. Nephrol. 28 (10) (2017) 2867–2878.
[43] Y.A. Hannun, R.M. Bell, Regulation of protein kinase-C by sphingosine and lysosphingolipids, Clin. Chim. Acta 185 (3) (1989) 333–346.
[44] A. Mima, Glomerular VEGF resistance induced by PKCdelta/SHP-1 activation and contribution to diabetic nephropathy, FASEB J. 26 (7) (2012) 2963-74.
[45] M. Kann, Genome-wide analysis of wilms' tumor 1-controlled gene expression in podocytes reveals key regulatory mechanisms, J. Am. Soc. Nephrol. 26 (9) (2015) 2097–2104.
[46] A.A. Morrison, New insights into the function of the Wilms tumor suppressor gene WT1 in podocytes, Am. J. Physiol. -Renal Physiol. 295 (1) (2008) F12–F17.
[47] D.M. Rasa, WT1 alternative splicing: role of its isoforms in neuroblastoma, J. Mol. Neurosci. 62 (2) (2017) 131–141.
[48] G. Guo, WT1 activates a glomerular-specific enhancer identified from the human nephrin gene, J. Am. Soc. Nephrol. 15 (11) (2004) 2851–2856.
[49] R.E. Palmer, WT1 regulates the expression of the major glomerular podocyte membrane protein Podocalyxin, Curr. Biol. 11 (22) (2001) 1805–1809.
[50] B.R. Dey, Repression of the transforming growth-factor-beta-1 gene by the wilms-tumor suppressor Wt1 gene-product, Mol. Endocrinol. 8 (5) (1994) 595–602.
[51] Y. Ye, Regulation of WT1 by phosphorylation: inhibition of DNA binding, alteration of transcriptional activity and cellular translocation, EMBO J. 15 (20) (1996) 5606-5615.
[52] A.H. Merrill Jr., V.L. Stevens, Modulation of protein kinase C and diverse cell functions by sphingosine—a pharmacologically interesting compound linking sphingolipids and signal transduction, Biochim. Biophys. Acta (1989) 1010(2): p. 131-9.
[53] I. Quack, PKC alpha mediates beta-Arrestin2-dependent nephrin endocytosis in hyperglycemia, J. Biol. Chem. 286 (15) (2011) 12959–12970.
[54] Y. Emoto, Proteolytic activation of protein kinase C delta by an ICE-like protease in apoptotic cells, EMBO J. 14 (24) (1995) 6148-56.
[55] U. Lenkkeri, Structure of the gene for congenital nephrotic syndrome of the Finnish type (NPHS1) and characterization of mutations, Am. J. Hum. Genet. 64 (1) (1999) 51–61.
[56] M. Kestila, Positionally cloned gene for a novel glomerular protein - nephrin - is mutated in congenital nephrotic syndrome, Mol. Cell 1 (4) (1998) 575–582.
[57] J. Hulkko, Neph1 is reduced in primary focal segmental glomerulosclerosis, minimal change nephrotic syndrome, and corresponding experimental animal models of adriamycin-

induced nephropathy and puromycin aminonucleoside nephrosis, Nephron Extra 4 (3) (2014) 146–154.
[58] S. Doublier, Nephrin expression is reduced in human diabetic nephropathy - Evidence for a distinct role for glycated albumin and angiotensin II, Diabetes 52 (4) (2003) 1023–1030.
[59] D. Veron, Overexpression of VEGF-A in podocytes of adult mice causes glomerular disease, Kidney Int. 77 (11) (2010) 989–999.
[60] K. Yamauchi, Screening and identification of substances that regulate nephrin gene expression using engineered reporter podocytes, Kidney Int. 70 (5) (2006) 892–900.
[61] X.S. Qin, Phosphorylation of nephrin triggers its internalization by raft-mediated endocytosis, J. Am. Soc. Nephrol. 20 (12) (2009) 2534–2545.
[62] C. Ponticelli, F. Locatelli, Glucocorticoids in the treatment of glomerular diseases pitfalls and pearls, Clin. J. Am. Soc. Nephrol. 13 (5) (2018) 815–822.
[63] L.L. Jiang, RNA sequencing analysis of human podocytes reveals glucocorticoid regulated gene networks targeting non-immune pathways, Sci. Rep. 6 (2016).
[64] P.J. Blackshear, Tristetraprolin and other CCCH tandem zinc-finger proteins in the regulation of mRNA turnover, Biochem. Soc. Trans. 30 (2002) 945–952.
[65] C.M. Brennan, J.A. Steitz, HuR and mRNA stability, Cell. Mol. Life Sci. 58 (2) (2001) 266–277.
[66] A.J. Snider, Inhibition of sphingosine kinase-2 in a murine model of lupus nephritis, PLoS ONE 8 (1) (2013).
[67] S. Mohammed, Examination of the role of sphingosine kinase 2 in a murine model of systemic lupus erythematosus, FASEB J. 33 (6) (2019) 7061–7071.
[68] K.J. French, Pharmacology and antitumor activity of ABC294640, a selective inhibitor of sphingosine kinase-2, J. Pharmacol. Exp. Ther. 333 (1) (2010) 129–139.
[69] A. Huwiler, Histamine increases sphingosine kinase-1 expression and activity in the human arterial endothelial cell line EA.hy 926 by a PKC-alpha-dependent mechanism, Biochim. Biophys. Acta 1761 (3) (2006) 367–376.
[70] L. Schaefer, Nephrin expression is increased in anti-Thy1.1-induced glomerulonephritis in rats, Biochem. Biophys. Res. Commun. 324 (1) (2004) 247–254.
[71] S.Y. Ren, PPAR alpha activation upregulates nephrin expression in human embryonic kidney epithelial cells and podocytes by a dual mechanism, Biochem. Biophys. Res. Commun. 338 (4) (2005) 1818–1824.
[72] H. Pavenstadt, Effect of nucleotides on the cytosolic free calcium activity and inositol phosphate formation in human glomerular epithelial cells, Br. J. Pharmacol. 107 (1) (1992) 189–195.
[73] M.A. Saleem, A conditionally immortalized human podocyte cell line demonstrating nephrin and podocin expression, J. Am. Soc. Nephrol. 13 (3) (2002) 630-8.
[74] H. Schmidt, R. Schmidt, G. Geisslinger, LC-MS/MS-analysis of sphingosine-1-phosphate and related compounds in plasma samples, Prostaglandins Other Lipid Mediat. 81 (2006) 162–170 (3-4).